The Neumann-Michell theory of ship waves

Francis Noblesse[1], **Fuxin Huang**[2], **Chi Yang**[2]

francis.noblesse@navy.mil , fhuang@gmu.edu , cyang@gmu.edu

[1] David Taylor Model Basin, NSWCCD, West Bethesda, MD, USA

[2] Dept of Computational and Data Sciences, George Mason University, Fairfax, VA, USA

This work was sponsored by the Office of Naval Research. Ms. Kelly Cooper is the technical monitor.

Introduction

The classical Neumann-Kelvin (NK) theory of linear potential flow about a ship hull that steadily advances along a straight path in calm water (of effectively infinite depth and lateral extent) expounded in [1,2] is reconsidered. The revised NK theory, called Neumann-Michell (NM) theory, expounded in [3] is summarized and applied.

The flow about the ship hull is observed from a moving system of orthogonal coordinates $\mathbf{X} \equiv (X, Y, Z)$ attached to the ship, and thus appears steady with flow velocity given by the sum of an apparent uniform current $(-V_s, 0, 0)$ opposing the ship speed V_s and the (disturbance) flow velocity due to the ship. The X axis is chosen along the path of the ship and points toward the ship bow. The Z axis is vertical and points upward, with the mean (undisturbed) free surface taken as the plane $Z=0$. Nondimensional coordinates $\mathbf{x} \equiv \mathbf{X}/L_s$, flow potential $\phi \equiv \Phi/(L_s V_s)$ and related flow velocity $\nabla\phi$ are defined in terms of the length L_s and the speed V_s of the ship. The Froude number is defined as $F \equiv V_s/\sqrt{g L_s}$ where g is the acceleration of gravity.

The Neumann-Kelvin (NK) and Neumann-Michell (NM) theories

The NM theory circumvents three major basic difficulties of the NK theory, as now briefly explained.

•1 A well-known basic 'technical' difficulty of the NK theory is the complexity of the Green function that satisfies the linearized Kelvin-Michell free-surface boundary condition and the radiation condition. This Green function is commonly expressed as the sum of a wave component W that is given by a Fourier superposition of elementary waves and satisfies the radiation condition, and a local-flow component L that is given by a somewhat complicated integral representation [4]. However, the local component L (and its gradient) can be well approximated by the simple analytical expression, valid in the entire flow field, given in [5] . Furthermore, calculations show that numerical predictions obtained using the simple analytical approximation given in [5] or the even simpler approximation, given by a combination of three elementary free-space Rankine sources, proposed in [6,7] do not differ significantly. The Green function $G(\widetilde{\mathbf{x}}\,;\mathbf{x})$, where $\mathbf{x} \equiv (x, y, z)$ and $\widetilde{\mathbf{x}} \equiv (\widetilde{x}, \widetilde{y}, \widetilde{z})$ stand for a source point and a flow field point, can therefore be greatly simplified as

$$G \equiv W + L \approx \frac{H(x-\widetilde{x})}{\pi F^2}\, \Im\mathrm{m} \int_{-t_\infty}^{t_\infty} dt\, \widetilde{\Lambda}\, \widetilde{\mathcal{E}}\, \mathcal{E} + L \quad \text{with} \quad 4\pi L \approx \frac{-1}{r} + \frac{1}{r_1} - \frac{2}{r_2} \tag{1}$$

The finite limits of integration $\pm t_\infty$ and the function $\widetilde{\Lambda}$ in the wave component filter physically unrealistic short waves. The elementary waves $\mathcal{E}$ and $\widetilde{\mathcal{E}}$ in the wave component W and the three elementary free-space Rankine sources in the local-flow component L are defined as

$$\mathcal{E} \equiv e^{\,(1+t^2)\,z/F^2 \,-\, i\sqrt{1+t^2}\,(x+t\,y)/F^2} \qquad \widetilde{\mathcal{E}} \equiv e^{\,(1+t^2)\,\widetilde{z}/F^2 \,+\, i\sqrt{1+t^2}\,(\widetilde{x}+t\,\widetilde{y})/F^2}$$

$$r \equiv \sqrt{h^2+(\widetilde{z}-z)^2} \quad r_1 \equiv \sqrt{h^2+(\widetilde{z}+z)^2} \quad r_2 \equiv \sqrt{h^2+(\widetilde{z}+z-F^2)^2} \quad \text{with} \quad h \equiv \sqrt{(\widetilde{x}-x)^2+(\widetilde{y}-y)^2}$$

The combination of three elementary free-space Rankine sources that approximate the local flow component L in (1) asymptotically satisfies the Kelvin-Michell free-surface boundary condition in both the nearfield and the farfield, and the linear superposition of elementary waves in the wave component W satisfies the Kelvin-Michell free-surface boundary condition and the radiation condition [4,8] . The Green function (1) and the straightforward regularization approach given in [5] lead to a practical, indeed particularly simple, mathematical flow representation. This flow representation only involves *ordinary continuous functions*, which can readily be integrated using straightforward Gaussian integration rules.

•2 Another well-known major fundamental difficulty of the NK theory expounded in [1,2] is that the NK boundary-integral flow representation involves a troublesome line integral around the ship waterline. Specifically, the NK theory expresses the flow potential $\widetilde{\phi}$ at a flow field point $\widetilde{\mathbf{x}}$ in terms of a surface integral over the mean wetted ship hull surface Σ^H and a line integral around the ship mean waterline Γ, as

$$\widetilde{\phi} = \int_{\Sigma^H} da\, (G\, n^x - \phi\, \mathbf{n}\cdot\nabla G) + F^2 \int_\Gamma d\ell\, (\phi\, G_x - G\, \phi_x)\, n^x/\sqrt{(n^x)^2+(n^y)^2} \tag{2}$$

Here, the unit vector $\mathbf{n} \equiv (n^x, n^y, n^z)$ is normal to the ship hull surface Σ^H and points outside the ship (into the water). The waves that stem from the waterline integral around Γ and the hull-surface integral over Σ^H are well known to largely cancel out, e.g. [5], which unavoidably causes a loss of numerical accuracy. This loss of accuracy is rendered more severe by the fact that the waterline integral around Γ involves flow evaluation at the mean free-surface plane $\widetilde{z} = 0$, which cannot be done accurately as noted below. However, the waterline

integral in the NK representation (2) can be eliminated, via a two-step process now briefly explained.

(i) A basic initial step in the NK theory considered since its initial formulation in [1,2] is that the linearized boundary condition at the free surface is enforced—ab initio—at the mean free-surface plane $z = 0$. However, this initial assumption ignores a *linear* contribution of the narrow band of the ship hull surface located between the actual free surface and the mean free-surface plane $z = 0$. In fact, the NK flow representation (2) does not correspond to a *consistent linear flow model*, for which the term $G\phi_x$ in (2) does not occur.

(ii) The term ϕG_x in (2) does appear within a consistent linear flow model, but this term can be eliminated using a mathematical transformation. The transformation essentially amounts to an integration by parts, based on a *vector* wave function $\mathbf{W} \equiv (0, W_z^x, -W_y^x)$ associated with the *scalar* wave component W in the Green function (1) via the relation $\nabla \times \mathbf{W} = \nabla W$.

The foregoing two steps eliminate the line integral around the ship waterline Γ in the NK flow representation (2). The corresponding Neumann-Michell flow representation, based on a consistent linear flow model and an integration by parts, expresses the flow potential $\widetilde{\phi}$ at a flow field point $\widetilde{\mathbf{x}}$ as the surface integral

$$\widetilde{\phi} \approx \int_{\Sigma^H} da\, [\, G\, n^x + (n^y W_y^x + n^z W_z^x)\, \phi_x - (\phi_y W_y^x + \phi_z W_z^x)\, n^x - \phi\, \mathbf{n} \cdot \nabla L\,] \tag{3}$$

over the mean wetted ship hull surface Σ^H. Numerical inaccuracies associated with the evaluation of the waterline integral, and its partial cancellation with the hull surface integral, in the NK flow representation (2) are then moot issues in the NM flow representation (3). The NM boundary integral equation (3) is significantly simplified if the local-flow component associated with the dipole distribution $\phi\, \mathbf{n} \cdot \nabla L$ is ignored, as justified for flow about a steadily advancing slender body [9]. This practical simplification yields a useful approximation.

•3 A third major basic difficulty that affects the NK theory, as well as the related NM modification, stems from the fact that while robust and accurate numerical evaluation of the Fourier integral that defines the wave component W in the Green function (1) is possible if $\widetilde{z} < 0$ (for flow field points $\widetilde{\mathbf{x}}$ strictly below the mean free-surface plane $\widetilde{z} = 0$), numerical evaluation is problematic for a flow field point $\widetilde{\mathbf{x}}$ at the mean free-surface plane because $\widetilde{\mathcal{E}} = 1$ if $\widetilde{z} = 0$ for every value of the Fourier variable t. Reconsideration of this essential difficulty of flow calculation methods based on the Green function (1), or a related Green function that satisfies the Kelvin-Michell free-surface boundary condition and the radiation condition, has resulted in an effective practical new approach. In this approach, the wave component is evaluated at the mean free surface using parabolic extrapolation and a physics-based filtering of short waves that treats the transverse waves aft of a ship bow wave differently from the bow wave; indeed, a ship bow wave typically is shorter, higher, sharper, and accordingly more affected by divergent waves, than waves aft of the bow wave.

Illustrative application to Wigley hull

Figs 1–3 depict solutions, given by an iterative solution procedure that only requires a few seconds using a PC, of the NM integral equation (3) for the Wigley parabolic hull. The dipole distribution $\phi\, \mathbf{n} \cdot \nabla L$ in (3) is ignored. The Green function given in [5] is used. The Wigley hull is approximated by 16,000 flat triangular panels.

The NM predictions (NM) agree well with experimental measurements, and yield significantly more realistic wave profiles and wave drag than the Hogner slender-ship approximation (SS), also shown in Figs 1-2. The results depicted in Figs 1–3 are encouraging and suggest that the NM theory may provide a useful practical method well suited for routine applications to ship design and hull-form optimization.

References

[1] Brard R (1972) The representation of a given ship form by singularity distributions when the boundary condition on the free surface is linearized. J. Ship Research 16:79-92

[2] Guevel P, Vaussy P, Kobus JM (1974) The distribution of singularities kinematically equivalent to a moving hull in the presence of a free surface. Il Shipbuilding Progress 21:311-324

[3] Noblesse F, Huang F, Yang C (submitted) The Neumann-Michell theory of ship waves

[4] Noblesse F (1981) Alternative integral representations for the Green function of the theory of ship wave resistance. J. Engineering Mathematics 15:241-265

[5] Noblesse F, Delhommeau G, Huang F, Yang C (2011) Practical mathematical representation of the flow due to a distribution of sources on a steadily-advancing ship hull. J. Engineering Mathematics 71:367-392

[6] Noblesse F, Yang C (2004) A simple Green function for diffraction-radiation of time-harmonic waves with forward speed, Ship Technology Research 51:35-52

[7] Yang C, Löhner R, & Noblesse F (2004) Comparison of classical and simple free-surface Green functions, Il J Offshore & Polar Engg 14:257-264

[8] Noblesse F, Yang C (2007) Elementary water waves, J Engineering Mathematics 59:277-299

[9] Noblesse F, Triantafyllou G (1983) Explicit approximations for calculating potential flow about a body, J. Ship Research 27:1-12

[10] Hogner E (1932) Hydromech. Probl. d. Schiffsantriebs, Herausgeg.v..Kempf u. E. Foerster, Hamburg 99-114

[11] Noblesse F (1983) A slender-ship theory of wave resistance. J. Ship Research 27:13-33

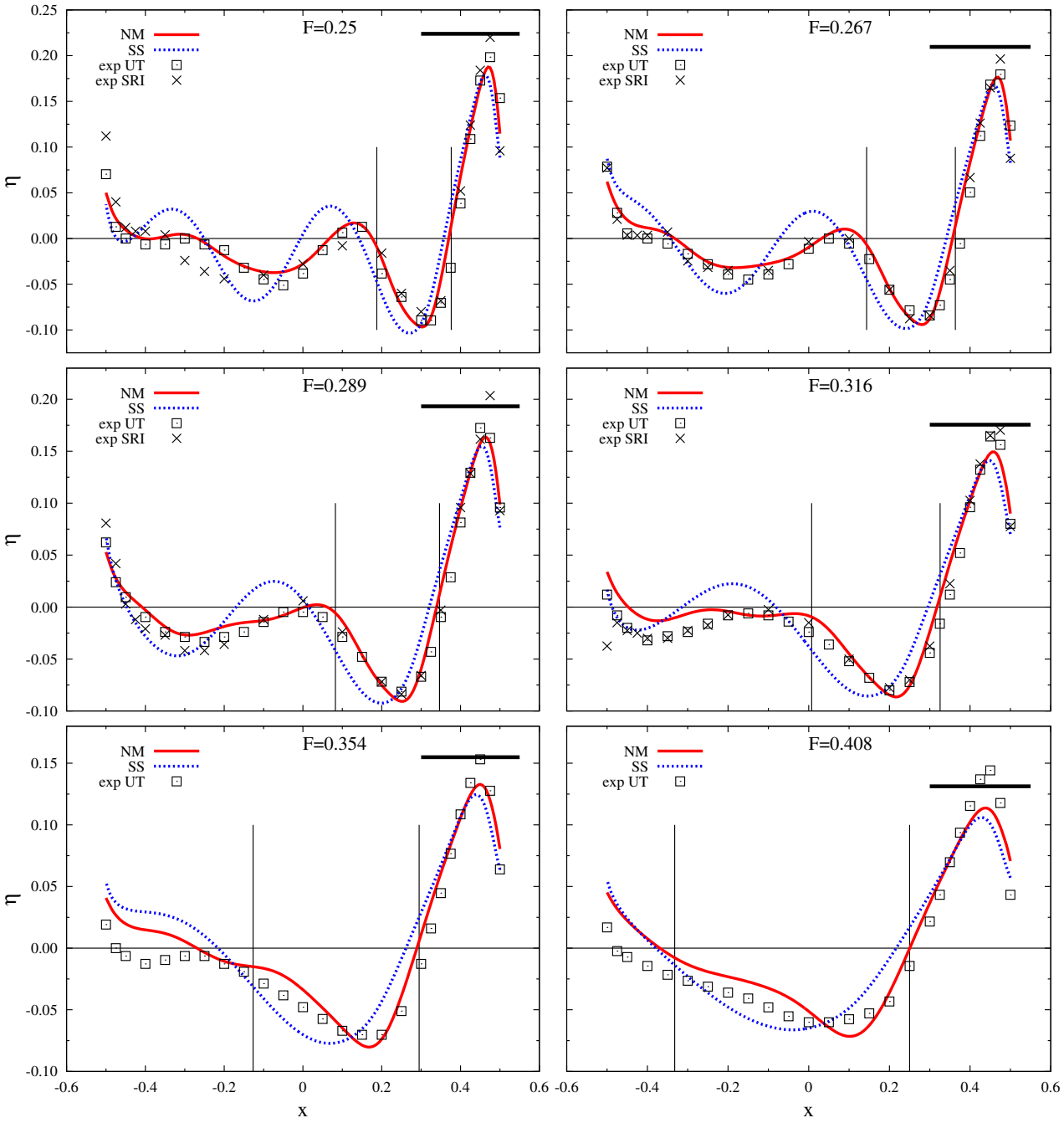

Figure 1: Wave profiles along the Wigley hull at F =0.25, 0.267, 0.289, 0.316, 0.354, 0.408 predicted by the Neumann-Michell (NM) theory and the related Hogner slender-ship (SS) approximation proposed in [10], or measured at the University of Tokyo (exp UT) and the Ship Research Institute (exp SRI). The horizontal line segments drawn for $0.3 \leq \widehat{x} \leq 0.55$ mark a theoretical estimate of the nonlinear bow wave height that corresponds to the linear bow wave height predicted by the NM theory. The two vertical lines mark the transition region between the 'short-wave' bow wave regime and the 'transverse-wave' regime aft of the bow wave. The bow waves predicted by the NM theory are realistic and in good agreement with experimental measurements. The NM bow waves are a bit higher than the SS bow waves, and are shifted slightly toward the stem $x = 0.5$. Aft of the bow wave, the NM theory predicts waves of significantly smaller amplitude than the SS approximation. Furthermore, the NM wave profiles are shifted toward the stem, in agreement with experimental measurements. Indeed, the NM profiles are more closely in phase with the experimental profiles than the SS profiles, consistently for every Froude number. Thus, the NM wave profiles are in significantly better agreement with experimental measurements than the SS profiles, in accordance with the fact that the boundary condition at the hull surface is satisfied in the NM theory but is only satisfied approximately in the Hogner slender-ship approximation. The SS and NM flow predictions are obtained in a few seconds per Froude number using a PC.

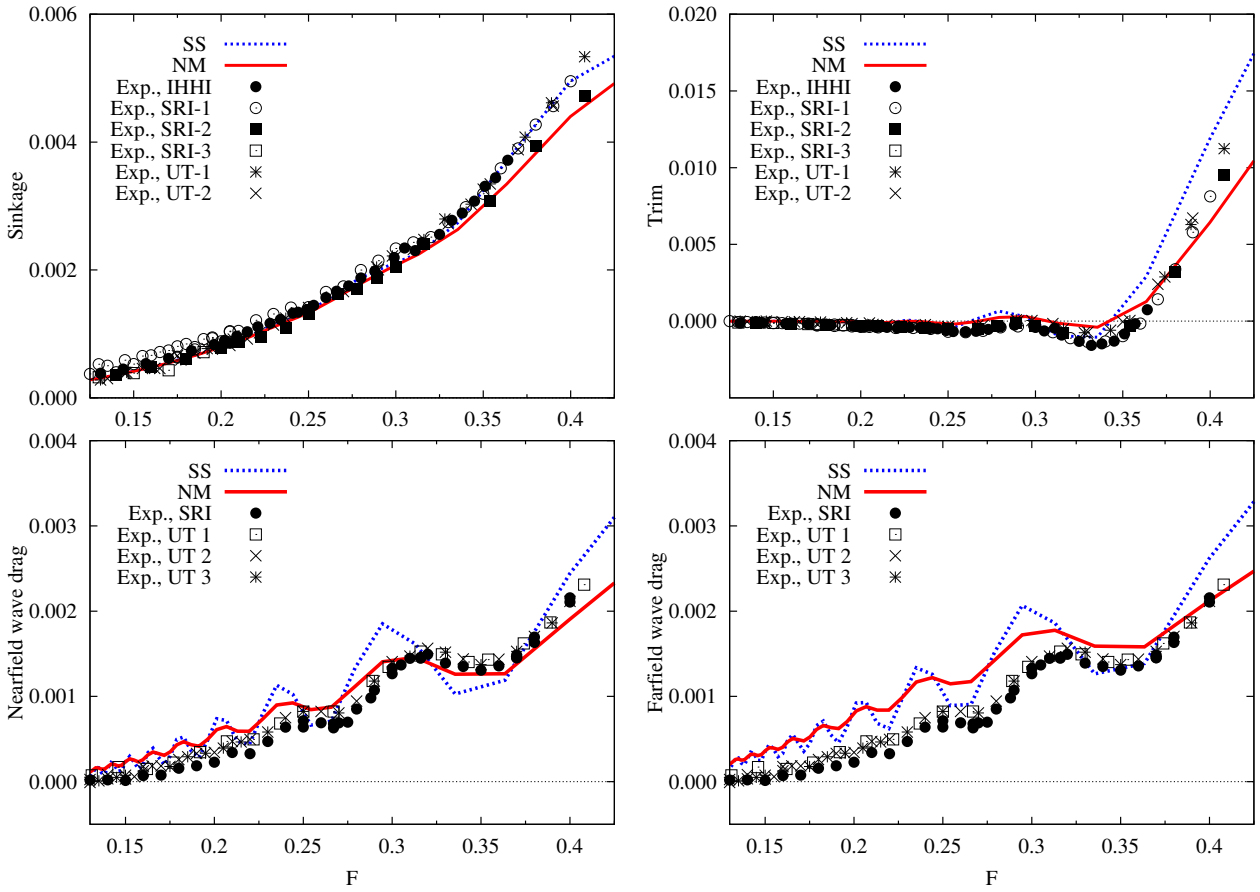

Figure 2: Experimental measurements and theoretical predictions, given by the Hogner slender-ship (SS) approximation or the Neumann-Michell (NM) theory, of sinkage (top left corner), trim (top right), nearfield wave drag (bottom left) and farfield (Havelock) wave drag (bottom right) for the Wigley hull. The NM wave drag is considerably less oscillatory, and in significantly better agreement with experimental measurements, than the SS wave drag. Thus, the excessive oscillations of the wave drag predicted by the classical Michell thin-ship approximation and the related slender-ship approximations proposed in [10,11] are not due to viscous or nonlinear effects as sometimes assumed in the literature, but are related to the boundary condition at the ship hull surface. This boundary condition is only approximately satisfied in the thin-ship or slender-ship approximations.

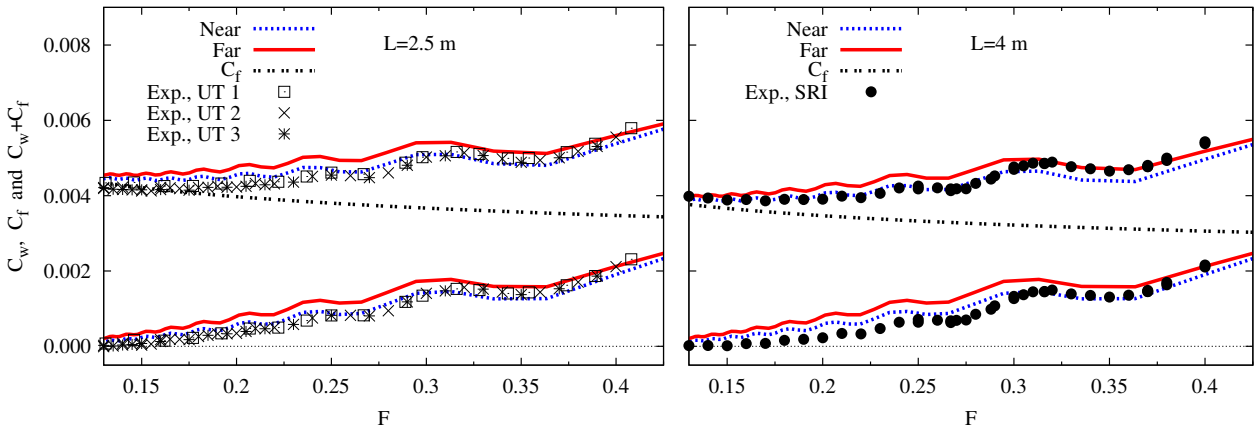

Figure 3: NM predictions of the nearfield and farfield wave drag (bottom curve), viscous drag C_f given by the ITTC friction-drag formula, and corresponding total drag given by the sum of the wave and friction drags.